CHEMISTRY OF
MATERIALS
Article

Chem. Mater. **2010,** *22,* 247–254 247
DOI:10.1021/cm9029616

Phosphine Oxide Derivatives as Hosts for Blue Phosphors: A Joint Theoretical and Experimental Study of Their Electronic Structure

Dongwook Kim,[†] Seyhan Salman,[†] Veaceslav Coropceanu,[†] Eric Salomon,[‡,∥]
Asanga B. Padmaperuma,[§] Linda S. Sapochak,[§,⊥] Antoine Kahn,[‡] and Jean-Luc Brédas*,[†]

[†]*School of Chemistry and Biochemistry & Center for Organic Photonics and Electronics, Georgia Institute of Technology, Atlanta, Georgia 30332-0400,* [‡]*Department of Electrical Engineering, Princeton University, Princeton, New Jersey 08544-5263, and* [§]*Energy and Environment Directorate, Pacific Northwest National Laboratory, Richland, Washington 99352.* [∥] *Current address: Université de Provence, Service 241, Campus de Saint-Jérôme, Avenue Escadrille Normandie Niémen, 13397 Marseille Cedex, France.* [⊥] *Current address: National Science Foundation, 4201 Wilson Blvd., Arlington, VA 22230.*

Received September 23, 2009. Revised Manuscript Received November 11, 2009

We report on a joint theoretical and experimental investigation of the electronic structure of a series of bis(diphenylphosphine oxide) derivatives containing a central aromatic core with high triplet energy. Such molecules can serve as host material in the emissive layer of blue electro-phosphorescent organic devices. The aromatic cores considered in the theoretical study consist of biphenyl, fluorene, dibenzofuran, dibenzothiophene, dibenzothiophenesulfone, or carbazole, linked to the two phosphoryl groups in either *para* or *meta* positions. With respect to the isolated core molecules, it is found that addition of the diphenylphosphine oxide moieties has hardly any impact on the core geometry and only slightly reduces the energy of the lowest triplet state (by, at most, ~0.2 eV). However, the diphenylphosphine oxide functionalities significantly impact the ionization potential and electron affinity values, in a way that is different for *para* and *meta* substitutions. Excellent comparison is obtained between the experimental UPS and IPES spectra of the *para* biphenyl and *meta* dibenzothiophene and dibenzothiophenesulfone compounds and the simulated spectra. In general, the phosphine oxide derivatives present triplet energies that are calculated to be at least 0.2 eV higher than those of currently widely used blue phosphorescent emitters.

I. Introduction

Phosphorescent organic light emitting diodes (PhOLEDs) are receiving a great deal of attention, because of their applications in full-color displays and large-area solid-state lighting.[1,2] To prevent concentration quenching of the luminescence, PhOLEDs generally present an emitting layer consisting of a guest phosphorescent emitter embedded in a host matrix; among several parameters, the device performance depends on the luminescence quantum efficiency of the light-emitting guest material and the ability of the host material to efficiently transfer charge/energy to the guest molecules. The development of suitable host materials for blue emitters has turned out to be a rather challenging task, partially because the host materials, in addition to good charge/energy-transporting properties, must display sufficiently high excited-state energies to prevent back energy transfer from the phosphorescent guest. Various host materials based, for instance, on carbazole or silane derivatives have been considered,[3−11] although issues related to device efficiency and/or lowering of device operating voltage remain. More recently, diphenylphosphine oxide (PO) derivatives of aromatic molecules with large optical gaps have emerged as another class of host materials for blue OLEDs.[12−18] By facilitating electron injection into the emitting layer,

---

*Author to whom correspondence should be addressed. E-mail: jean-luc.bredas@chemistry.gatech.edu.

(1) Baldo, M. A.; O'Brien, D. F.; You, Y.; Shoustikov, A.; Sibley, S.; Thompson, M. E.; Forrest, S. R. *Nature* **1998**, *395*, 151.
(2) Baldo, M. A.; Lamansky, S.; Burrows, P. E. *Appl. Phys. Lett.* **1999**, *75*, 4.
(3) Holmes, R. J.; D'Andrade, B. W.; Forrest, S. R.; Ren, X.; Li, J.; Thompson, M. E. *Appl. Phys. Lett.* **2003**, *83*, 3818.
(4) Holmes, R. J.; Forrest, S. R.; Tung, Y.-J.; Kwong, R. C.; Brown, J. J.; Garon, S.; Thompson, M. E. *Appl. Phys. Lett.* **2003**, *82*, 2422.
(5) Tokito, S.; Iijima, T.; Suzuri, Y.; Kita, H.; Tsuzuki, T.; Sato, F. *Appl. Phys. Lett.* **2003**, *83*, 569.
(6) Ren, X.; Li, J.; Holmes, R. J.; Djurovich, P. I.; Forrest, S. R.; Thompson, M. E. *Chem. Mater.* **2004**, *16*, 4743.
(7) Yeh, S.-J.; Wu, M.-F.; Chen, C.-T.; Song, Y.-H.; Chi, Y.; Ho, M.-H.; Hsu, S.-F.; Chen, C. H. *Adv. Mater.* **2005**, *17*, 285.
(8) Tsai, M.-H.; Lin, H.-W.; Su, H.-C.; Ke, T.-H.; Wu, C.-c.; Fang, F.-C.; Liao, Y.-L.; Wong, K.-T.; Wu, C.-I. *Adv. Mater.* **2006**, *18*, 1216.
(9) Agata, Y.; Shimizu, H.; Kido, J. *Chem. Lett.* **2007**, *36*, 316.
(10) Tsai, M.-H.; Hong, Y.-H.; Chang, C.-H.; Su, H.-C.; Wu, C.-C.; Matoliukstyte, A.; Simokaitiene, J.; Grigalevicius, S.; Grazulevicius, J. V.; Hsu, C.-P. *Adv. Mater.* **2007**, *19*, 862.
(11) Williams, E. L.; Haavisto, K.; Li, J.; Jabbour, G. E. *Adv. Mater.* **2007**, *19*, 197.
(12) Burrows, P. E.; Padmaperuma, A. B.; Sapochak, L. S.; Djurovich, P.; Thompson, M. E. *Appl. Phys. Lett.* **2006**, *88*, 183503.
(13) Vecchi, P. A.; Padmaperuma, A. B.; Qiao, H.; Sapochak, L. S.; Burrows, P. E. *Org. Lett.* **2006**, *8*, 4211.
(14) Padmaperuma, A. B.; Sapochak, L. S.; Burrows, P. E. *Chem. Mater.* **2006**, *18*, 2389.
(15) Sapochak, L. S.; Padmaperuma, A. B.; Vecchi, P. A.; Qiao, H.; Burrows, P. E. *Proc. SPIE* **2006**, *6333*, 57.
(16) Sapochak, L. S.; Padmaperuma, A. B.; Vecchi, P. A.; Cai, X.; Burrows, P. E. *Proc. SPIE* **2007**, *6655*, 65506.
(17) Cai, X.; Padmaperuma, A. B.; Sapochak, L. S.; Vecchi, P. A.; Burrows, P. E. *Appl. Phys. Lett.* **2008**, *92*, 083308.
(18) Sapochak, L. S.; Padmaperuma, A. B.; Cai, X.; Male, J. L.; Burrows, P. E. *J. Phys. Chem. C* **2008**, *112*, 7989.

devices exploiting PO derivatives can present rather low operating voltages.[13−15] In addition, the lowest triplet states of POs are consistently higher in energy than that of iridium(III) bis(4,6-difluorophenyl)pyridinato-*N*,$C^{2\prime}$) picolinate (FIrpic), which is widely used as a blue phosphor.

The photophysical properties of the diphenylphosphine oxide derivatives have been extensively studied.[12−18] It was shown, for instance, that the phosphoryl groups (−P═O) act as effective breaking points of π-conjugation between the core arylene segment and the outer phenyl groups; as a result, the electronic structure of these compounds are consistently observed to be very similar to those of the central moiety.[13,15] However, despite these extensive experimental investigations and some earlier electronic-structure calculations (indicating that the frontier molecular orbitals (FMOs) in the PO derivatives are localized on the core),[13−16] a comprehensive study of the relationship between structure and electronic properties in PO compounds is still missing.

Here, we describe the results of density functional theory (DFT) calculations performed on several representative PO molecules, in addition to, for the sake of comparison of guest−host triplet energies, two widely used blue-emitting phosphors: platinum(II) (2-(4′,6′-difluorophenyl)pyridinato-*N*,$C^{2\prime}$)(2,4-pentanedionato-*O*,*O*) (FPt1) and FIrpic. We discuss, in particular, the influence of the phosphoryl units and substitution pattern on the modulation of the molecular ionization potential (IP) and electron affinity (EA) energies, as well as the effect of the substituents on the triplet energy of the core segment. In addition, we report the ultraviolet photoelectron spectroscopy (UPS) and inverse photo-emission spectroscopy (IPES) data for the *para*-biphenyl and *meta*-dibenzothiophene and *meta*-dibenzothiophenesulfone compounds.

II. Experimental Details

(a). Computational Methodology. The chemical structures of the bis(diphenylphosphine oxide) derivatives and blue phosphors investigated theoretically in this work are depicted in Figures 1 and 2, respectively. The aromatic cores consist of biphenyl, fluorene, dibenzofuran, dibenzothiophene, dibenzothiophenesulfone, or carbazole. The relative positions of the phosphoryl units, i.e., *para* (on the C2 positions in Figure 1) versus *meta* (on the C3 positions) are determined with respect to the carbon atoms bridging the phenylene rings (the Cb positions). The DFT calculations were performed with the B3LYP functional and the split-valence SV(P) basis set as implemented in the TURBOMOLE program (Version 5.9).[19−21] The molecular geometries were optimized using spin-restricted DFT calculations for the ground state (S_0) and spin-unrestricted DFT calculations for the lowest triplet excited states (T_1). All optimized geometries were confirmed to be minima on the potential energy surfaces by performing vibrational frequency calculations. Adiabatic triplet energies were obtained by means of the ΔSCF method on the basis of the optimized structures of the S_0 and T_1 states; zero-point vibrational energy (ZPVE) corrections were also taken into account. To shed more light on the nature of the triplet states of the core units and their PO derivatives, natural transition orbital (NTO) analyses[22,23] were performed with the time-dependent (TD) DFT approach, using the T_1 optimized geometries.

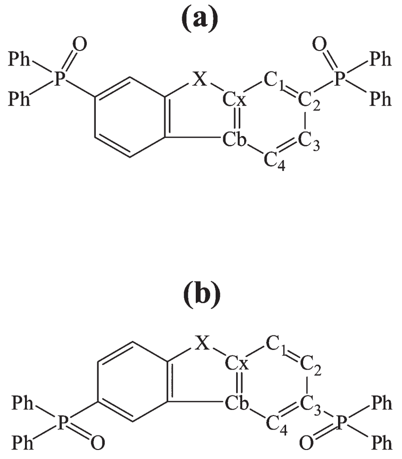

Figure 1. Chemical structures of the bis(diphenylphosphine oxide) derivatives with cores consisting of biphenyl (X = 2H), dibenzofuran (X = O), dibenzothiophene (X = S), dibenzothiophenesulfone (X = SO_2), carbazole (X = NH), and fluorene (X = CH_2): (a) [*p*,*p*]-derivatives and (b) [*m*,*m*]-derivatives.

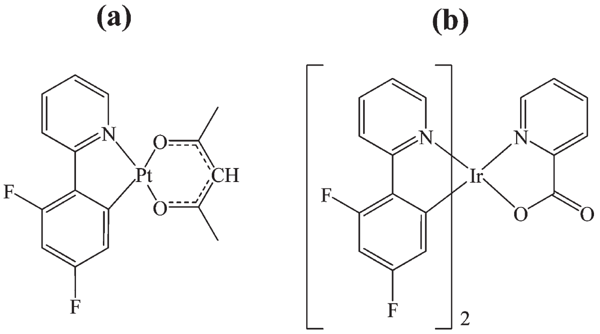

Figure 2. Chemical structures of representative blue phosphors: (a) platinum(II) (2-(4′,6′-difluorophenyl)pyridinato-*N*,$C^{2\prime}$)(2,4-pentanedionato-*O*,*O*) (FPt1); and (b) iridium(III) bis(4,6-difluorophenyl)pyridinato-*N*,$C^{2\prime}$) picolinate (FIrpic).

In addition, to better assess the relative charge-injection properties into POs and phosphors, the adiabatic ionization potentials (IPs) and electron affinities (EAs) (defined here as energy differences between the relaxed neutral state and cationic/anionic state, respectively) also were determined. Simulation of the UPS and IPES spectra was performed following the standard procedure outlined earlier,[24] which effectively allows solid-state polarization effects to be taken into account; the calculated density of states was convolved with a Gaussian function of full width at half-maximum set at 0.80 eV for the empty states and 0.55 eV for the filled states; then, a shift along the energy axis was applied to the entire spectrum to match against experimental peaks.

(b). Synthesis Aspects. The synthesis and characterization of 4,4′-bis(diphenylphosphoryl) biphenyl ([*p*,*p*]-biphenyl PO) was

---

(19) Bauernschmitt, R.; Ahlrichs, R. *Chem. Phys. Lett.* **1996**, *256*, 454.
(20) Bauernschmitt, R.; Ahlrichs, R. *Chem. Phys. Lett.* **1997**, *264*, 573.
(21) Furche, F.; Ahlrichs, R. *J. Chem. Phys.* **2002**, *117*, 7433.
(22) Martin, R. L. *J. Chem. Phys.* **2003**, *118*, 4775.
(23) Batista, E. R.; Martin, R. L. Natural transition orbitals. In *Encyclopedia of Computational Chemistry*; Schleyer, P. v. R., Allinger, N. L., Clark, T., Gasteiger, J., Kollman, P. A., Schaefer, H. F. I., Schreiner, P. R., Eds.; Wiley: Chichester, U.K., 2004.
(24) Chan, C. K.; Kim, E.-G.; Brédas, J.-L.; Kahn, A. *Adv. Funct. Mater.* **2006**, *16*, 831.

Table 1. Geometric Parameters of Fluorene and Its Bis(diphenylphosphine oxide) Derivatives in the Ground State[a]

	core	[*m*,*m*]-PO	[*p*,*p*]-PO	Expt ([*p*,*p*]-PO)[b]
R(Cx−X[=CH$_2$]) (Å)	1.516	1.515	1.515	1.53/1.52
R(Cb−Cb) (Å)	1.472	1.472	1.469	1.47
R(Cx−Cb) (Å)	1.414	1.413	1.414	1.40/1.41
R(Cx−C1) (Å)	1.394	1.393	1.392	1.39/1.38
R(Cb−C4) (Å)	1.400	1.400	1.400	1.39/1.39
R(C1−C2[*para*-]) (Å)	1.402	1.402	1.408	1.40/1.40
R(C4−C3[*meta*-]) (Å)	1.399	1.405	1.400	1.38/1.39
R(C2−C3) (Å)	1.402	1.407	1.408	1.40/1.39
R(C2,3-P) (Å)		1.836	1.834	1.80/1.81
R(P−O) (Å)		1.507	1.508	1.49/1.49
∠XCxCb (°)	109.99	110.04	110.04	110.8/111.0
∠CbCbCx (°)	108.56	108.52	108.54	108.7/108.3
∠CxC1C2 (°)	119.11	119.14	119.28	118.7/119.2
∠C1C2C3 (°)	120.52	120.77	120.02	120.0/120.1
∠C2C3C4 (°)	120.61	120.09	120.82	121.4/121.2
ϕ([C2C3]P=O) (°)		155.71	−156.63	−165.4/-19.9

[a] Refer to Figure 1 for atom labeling. [b] The molecule actually studied in the experiment is 2,7-bis(diphenylphosphine oxide)-9,9-dimethyl-fluorene, i.e., it has two methyl groups on the bridging carbon atom of the fluorene moiety. See ref 14.

reported previously[14] and details for 2,8-bis(diphenylphosphoryl) dibenzothiophene ([*m*,*m*]- dibenzothiophene PO), and 2,8-bis(diphenylphosphoryl) dibenzothiophene-5′,5″-dioxide ([*m*,*m*]- dibenzothiophenesulfone PO) will be reported elsewhere. The PO compounds were purified by gradient temperature vacuum sublimation twice prior to experimental studies.

(c). UPS and IPES Characterizations. Experiments were performed in a dual-chamber ultrahigh vacuum (UHV) system equipped for organic film deposition and electron spectroscopy. The substrates used in this series of experiments consisted of Au(50 nm)/Ti(5 nm)/Si sonicated in acetone and methanol and introduced without further treatment in the UHV system. PO films (5−6 nm thick) were evaporated in the growth chamber (based pressure = 10^{-9} Torr) from heated crucibles containing PO powder. The samples were then transferred under UHV to the analysis chamber (base pressure = 10^{-10} Torr) for UPS and IPES analysis.

UPS was done with the He(I) (21.22 eV) and He(II) (40.8 eV) photon lines of a helium discharge lamp and a cylindrical mirror analyzer for electron detection. The overall resolution in UPS was 0.15 eV. IPES was performed in the isochromat mode using a low-energy electron gun and a fixed-photon energy detector.[25] Resolution in IPES was 0.45 eV. All energy scales were referenced to the Fermi level measured with both techniques on the bare gold substrate. The vacuum level was obtained from the secondary-electron cutoff measured in the low-kinetic-energy region of the He(I) spectra. Electron affinity (EA) and ionization potential (IP) were conventionally defined as the energy difference between the vacuum level and the leading edge of the occupied states and unoccupied states, respectively.[26]

III. Results and Discussion

(a). Geometry: Core Molecules Versus Their PO Derivatives. Table 1 collects the main geometric parameters in the ground state of the fluorene-based PO. The theoretical values are in very good agreement with the experimental data from ref 14, in particular for the core. As seen from Table 1, the geometric parameters of the core are hardly affected by the introduction of the PO groups; the bond distances change by less than 0.01 Å and the bond angles change by less than 0.5°. These negligible geometric modifications reflect that the phosphoryl units serve as effective breaking points of π-conjugation between the core and the outer phenyl rings. Similar results are found when comparing the optimized T_1-state geometries of fluorene and its PO derivatives; the differences in bond distances and angles of the fluorene unit remain lower than 0.01 Å and 0.7°, respectively (see Table 2). The nearly identical T_1-state geometries of the core indicate that the PO substituents have little impact on the orbitals associated with the $S_0 \leftrightarrow T_1$ transition; hence, the triplet transitions of fluorene-based POs are expected to be of the same nature as those of fluorene itself. The same trends are found for both the ground state and T_1 state in all the other PO systems examined here (see also Tables S1 and S2 in the Supporting Information for the ground-state and lowest triplet-state geometries of dibenzofuran and its PO derivatives).

Table 2. Geometric Parameters of Fluorene and Its Bis(diphenylphosphine oxide) Derivatives in the Lowest Triplet State[a]

	core	[*m*,*m*]-PO	[*p*,*p*]-PO
R(Cx−X[=CH2]) (Å)	1.520	1.520	1.519
R(Cb−Cb) (Å)	1.383	1.384	1.385
R(Cx−Cb) (Å)	1.472	1.472	1.468
R(Cx−C1) (Å)	1.367	1.369	1.366
R(Cb−C4) (Å)	1.456	1.450	1.451
R(C1−C2[*para*-]) (Å)	1.432	1.429	1.438
R(C4−C3[*meta*-]) (Å)	1.375	1.377	1.373
R(C2−C3) (Å)	1.427	1.437	1.436
R(C2,3-P) (Å)		1.836	1.822
R(P−O) (Å)		1.507	1.508
∠XCxCb (°)	108.97	109.15	108.99
∠CbCbCx (°)	109.68	109.58	109.66
∠CxC1C2 (°)	119.60	119.82	119.76
∠C1C2C3 (°)	120.43	120.59	119.66
∠C2C3C4 (°)	121.56	120.86	121.70
ϕ([C2C3]PO) (°)		161.53	−156.45

[a] Refer to Figure 1 for atom labeling.

Interestingly, the calculated orientations of the phosphoryl units in the fully optimized geometries are different from those coming from crystallographic data; in the case of the [*p*,*p*]-fluorene PO, for instance, the dihedral angles between the plane of the fluorene core and the P=O bonds are −19.9° and −165.4° in the crystal,[14] while the DFT calculations lead to an almost-parallel orientation of the P=O bonds, −156.6° for both. For a ground-state geometry with the P=O bonds oriented in the same way as in the experimental structure, the corresponding angles are calculated to be −24.0° and −156.4°. These two isomers present nearly identical stabilities as their total energy difference is ~6 meV (ca. 70 K). As a result, the energies and characteristics of the HOMO and LUMO levels are practically the same for both conformations (the HOMO and LUMO energies differ by 7 and 18 meV, respectively; hence, the energy gaps between HOMO and LUMO differ by only 11 meV).

The fact that only PO molecules with antiparallel P=O bonds are found in the crystal can be attributed to

---

(25) Wu, C. I.; Hirose, Y.; Sirringhaus, H.; Kahn, A. *Chem. Phys. Lett.* **1997**, *272*, 43.

(26) Cahen, D.; Kahn, A. *Adv. Mater.* **2003**, *15*, 271.

Table 3. Calculated HOMO and LUMO Energies in the Ground State of the Phosphine Oxide and Phosphorescent Molecules[a]

	Core		[*p*,*p*]-POs		[*m*,*m*]-POs	
X	HOMO	LUMO	HOMO	LUMO	HOMO	LUMO
2H	−6.20	−0.90	−6.54	−1.60	−6.45	−1.28
CH_2	−5.92	−0.92	−6.28	−1.61	−6.21	−1.29
O	−6.17	−1.13	−6.49	−1.78	−6.50	−1.54
S	−5.89	−1.13	−6.18	−1.78	−6.27	−1.52
SO_2	−6.76	−1.94	−6.88	−2.34	−6.93	−2.26
NH	−5.60	−0.85	−5.97	−1.59	−5.97	−1.24
NH-Br[b]			−5.98[b]	−1.34[b]	−5.81[b]	−1.37[b]
FPt1	−5.82	−1.88				
FIrpic	−5.61	−1.87				

[a] All energies are expressed in units of eV. [b] The molecules here correspond to the dibromo derivatives of carbazole.

intermolecular interactions (absent in the present DFT calculations conducted on single molecules). As a matter of fact, intermolecular hydrogen-bonding ($P{=}O\cdots H{-}C$) and edge-to-face $C{-}H\cdots\pi$ interactions are significant in the [*p*,*p*]-fluorene PO crystal; the former are likely responsible for the antiparallel orientations of the phosphoryl groups, as discussed previously.[13] As a matter of fact, the optimization of the P=O bond orientations in the [*m*,*m*]-dibenzofuran PO molecule (25.1° for both P=O groups) is also different from what is found in the crystal (79.1° and 83.5°; see Table S1 in the Supporting Information); again, the differences can be attributed to the intermolecular interactions present in the crystal, which, in this case, also include $\pi-\pi$ stacking interactions.[13]

(b). HOMO/LUMO Energies and IPs/EAs: Impact on the Charge-Injection Properties. Previous experimental studies have demonstrated that the use of PO derivatives was beneficial in lowering the device operating voltage; however, it remains unclear whether this is a consequence of reduced electron injection barriers or enhanced electron transport properties (or both).[12−16] Since blue OLEDs with PO hosts are still observed to suffer from unbalanced charge injections,[16−18] it is worth investigating how the PO substitutions can affect the charge-injection properties via modulation of the energies of the frontier MOs (HOMOs and LUMOs) and the IP/EA values.

The calculated HOMO and LUMO energies in the ground state of the core molecules and their PO derivatives are listed in Table 3. As expected,[27] the introduction of electron-withdrawing substituents stabilizes both the HOMO and LUMO levels of the parent molecule. However, for [*p*,*p*]-POs, the LUMO stabilizations are approximately twice as large as those of the HOMOs (0.65−0.74 eV vs 0.29−0.37 eV) while for [*m*,*m*]-POs, the HOMO and LUMO levels stabilize in nearly the same way (0.25−0.38 eV and 0.37−0.41 eV, respectively); note that these values do not include the $X = SO_2$ compounds, to which we will turn later. Interestingly, in an earlier theoretical work on carbazole versus dibromo-substituted carbazole,[28] the calculated trends were the opposite: The HOMO and LUMO stabilizations were calculated to be similar in the case of *para* substitutions, while the LUMO stabilizations were found to be twice as large as the HOMO stabilization in the case of *meta* substitutions (see Table 3). Given that both phosphoryl and bromide groups present an inductive electron-withdrawing nature, these contrasting trends can be attributed to their dissimilar mesomeric characteristics, i.e., an electron-withdrawing nature for the phosphoryl group versus an electron-donating nature for bromide. As seen in Figure 3, for example, in the case of carbazole, the LUMO has significant contribution from the *para* carbons (C2 positions), but negligible contribution from the *meta* carbons (C3 positions), while the opposite is true for the HOMO. Hence, the mesomeric effect, for instance on the LUMO, is expected to be stronger for *para* substitutions than for *meta* substitutions. This is confirmed by an analysis of the contributions of the P=O groups or Br atoms to the HOMO and LUMO charge distributions;[29] for example, in the case of the carbazole-based PO compounds, the contributions from the P=O groups for *para* and *meta* substitutions are calculated to be 0.4 and 3.5%, respectively, in the case of the HOMO, and 6.0 and 1.0%, respectively, in the case of the LUMO. Keeping this feature in mind, in conjunction with the well-established fact that an electron-withdrawing (electron-donating) group stabilizes (destabilizes) the LUMO (HOMO) level more strongly through mesomeric effects, the correlation diagrams shown in Figure 3 make full sense. These diagrams also confirm that the inductive effects due to the Br atoms or P=O groups dominate over their mesomeric effects.

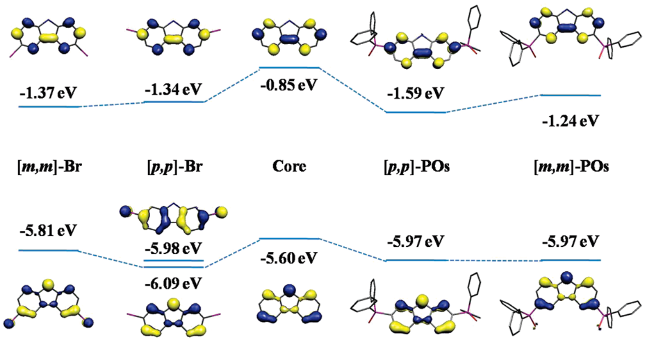

Figure 3. Illustration of the HOMO and LUMO wave functions and energies in the ground state of the carbazole molecule and its bis-(diphenylphosphine oxide) and dibromo derivatives. The HOMO-1 level of the [*p*,*p*]-Br derivative is also shown.

Turning now to the $X = SO_2$ compounds, we note that the presence in the core moiety of the highly electron-withdrawing $-SO_2$ group decreases the impact of the addition of the phosphoryl substituents. The HOMO energies decrease by 0.12 and 0.17 eV upon *para* and *meta* substitutions, respectively, and the LUMO energies decrease by 0.40 and 0.32 eV, respectively.

Having gained an understanding of the evolution of the HOMO and LUMO energies upon substitution, we now turn to a discussion of the IPs and EAs of the PO

---

(27) Cornil, J.; dos Santos, D. A.; Beljonne, D.; Brédas, J.-L. *J. Phys. Chem.* **1995**, *99*, 5604.

(28) Marsal, P.; Avilov, I.; da Silva Filho, D. A.; Brédas, J.-L.; Beljonne, D. *Chem. Phys. Lett.* **2004**, *392*, 521.

(29) We performed Löwdin population analysis on each frontier molecular orbitals for bromide and PO derivatives of carbazole.

Table 4. Ionization Potentials (IPs) and Electron Affinities (EAs) of the Phosphine Oxide and Phosphorescent Molecules[a]

	Core		[*p*,*p*]-POs		[*m*,*m*]-POs	
X	IP	EA[b]	IP	EA[b]	IP	EA[b]
2H	7.73	0.47	7.55	−0.72	7.52	−0.30
CH_2	7.49	0.58	7.36	−0.62	7.36	−0.24
O	7.95	0.42	7.53	−0.76	7.62	−0.43
S	7.57	0.37	7.49	−0.78	7.37	−0.43
SO_2	8.30	−0.50	7.88	−1.33	7.99	−1.18
NH	7.25	0.68	7.23	−0.59	7.14	−0.20
FPt1	7.20	−0.50				
FIrpic	6.68	−0.68				

[a] All energies are in eV. [b] EAs are defined as E(anionic state)-E(neutral state).

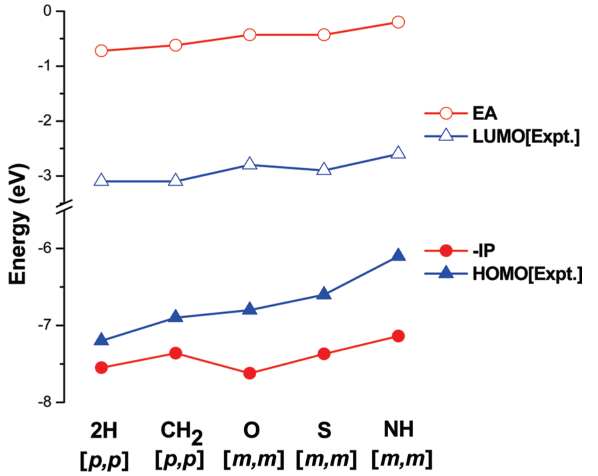

Figure 4. Comparison between the calculated IP and EA values and the experimental data for the bis(diphenylphosphine oxide) derivatives with X = 2H [*p*,*p*]; CH2 [*p*,*p*]; O [*m*,*m*]; S [*m*,*m*]; and NH [*m*,*m*]. The choice of the substitution pattern is related to the availability of experimental data. Note that experimental result for NH [*m*,*m*] corresponds to the *N*-ethyl derivative. See text and refs 15 and 16 for details regarding the experimental measurements.

derivatives and their core units. The results of the calculations are collected in Table 4 and compared with cyclic voltammetry data in Figure 4. It is important to note that the reported experimental EA energies are estimated from measured reduction potentials, whereas the "IP" energies are actually obtained from a combination of the EA values and lowest optical transitions (see refs 15 and 16 for details). Thus, the "IP" energies determined in this way must be considered with caution; indeed, the transport gap values do not directly correspond to the optical gap values, because of the contribution from the exciton binding energy in the latter. The calculated and experimental EA values correlate very well, with the DFT results reproducing the trends observed among the *para* compounds and among the *meta* compounds, as well as between *para* and *meta* compounds. In the case of the IP values, the calculations provide the right trends among the *para* compounds and among the *meta* compounds; the slight discrepancy found when comparing *para* and *meta* derivatives suggests that the exciton binding energies might be somewhat different in the two series of compounds.

To obtain a more-complete comparison of the electronic-structure data between theory and experiment,

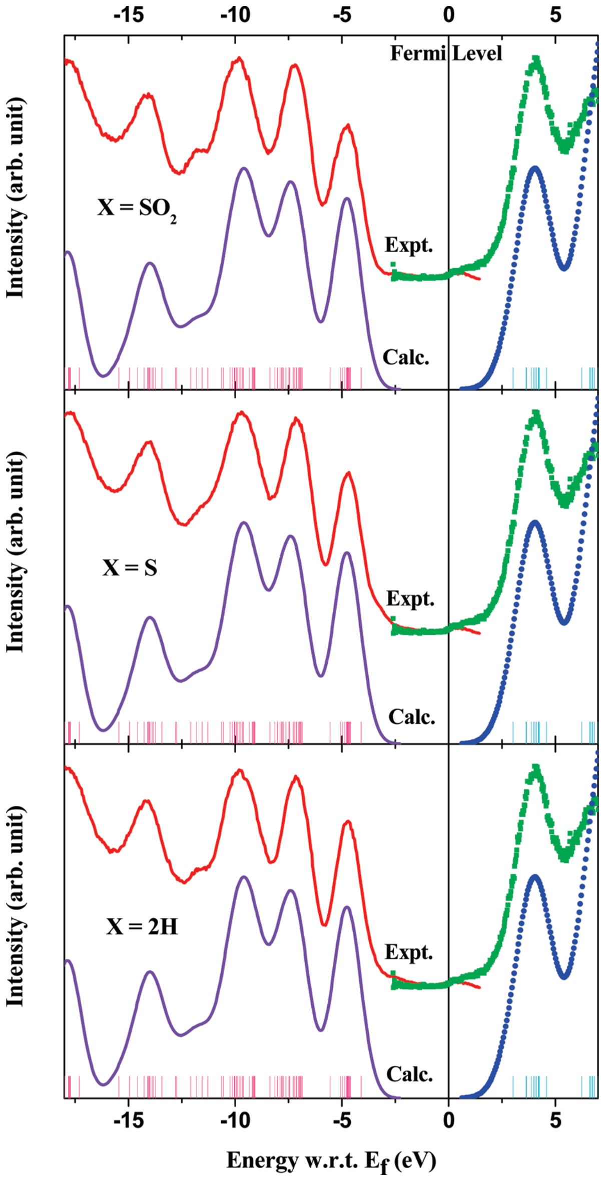

Figure 5. Experimental and simulated UPS and IPES spectra for the [*p*,*p*]-biphenyl (X = 2H), [*m*,*m*]-dibenzothiophene (X = S), and [*m*,*m*]-dibenzothiophenesulfone (X = SO_2) bis(phosphine oxide) derivatives.

UPS and IPES measurements were conducted for three PO derivatives: [*p*,*p*]-biphenyl, [*m*,*m*]-dibenzothiophene, and [*m*,*m*]-dibenzothiophenesulfone. The agreement between the experimental and simulated spectra is truly remarkable, both across the occupied (UPS) and unoccupied (IPES) states (see Figure 5); this agreement allows an accurate assessment of the origin of the various experimental peaks. Not surprisingly, given the similarities in the overall chemical structures of the three compounds, the UPS and IPES spectra look very much alike. The UPS IP values and IPES EA values are collected in Table 5, together with the corresponding DFT values calculated for the isolated molecules. Again, the calculations reproduce the experimental trends very well, when proper account is taken of the experimental uncertainties. For instance, the IPES data point to a decrease in electron affinity by some 0.4 eV when going from the [*p*,*p*]-biphenyl derivative to the [*m*,*m*]-dibenzothiophene

Table 5. Comparison between the DFT and UPS/IPES Experimental IP and EA Values for the [*p*,*p*]-biphenyl, [*m*,*m*]-dibenzothiophene, and [*m*,*m*]-dibenzothiophenesulfone bis(phosphine oxide) Compounds

	IP (eV)		EA (eV)	
X	theory	UPS	theory	IPES
2H	7.55	7.29 ± 0.2	−0.72	−2.9 ± 0.2
S	7.37	7.49 ± 0.2	−0.43	−2.5 ± 0.2
SO_2	7.99	7.52 ± 0.2	−1.18	−3.1 ± 0.2

derivative; the DFT calculations provide for a very similar decrease (0.3 eV). The comparison between theoretical and experimental IP trends is not as good. The origin of this small discrepancy is unclear, but could be related to the intensity shoulder at the very top of the valence states, especially on the X = S spectrum. The theoretical simulation clearly indicates that this density is not intrinsic to the compound and is likely related to defects, possibly related to the spectroscopy. Such defects could slightly affect the measured HOMO position.

It is useful to point out that the IP of FIrpic is calculated to be smaller than those of the PO derivatives by 0.5−1.2 eV; this is consistent with the experimental observation that holes preferentially inject into (and are trapped on) FIrpic rather than into the POs.[12−18] However, it is less clear that FPt1 could be used as such an injection/trapping site for holes, since its IP is 0.5 eV larger than for FIrpic and becomes comparable to those of some of the PO derivatives (the latter are sufficiently large to provide for hole-blocking properties).

(c). Lowest Triplet State. Efficient PhOLEDs require that the back energy transfer from guest to host be suppressed. Thus, the triplet energy of the host should be larger than that of the guest, which means that, for (deep) blue OLEDs, the host T_1 energy should be on the order of, or larger than, ~3 eV. Table 6 lists the adiabatic triplet transition energies (energy difference between the relaxed T_1- and S_0-states) of the PO derivatives, as well as of FPt1 and FIrpic. The DFT estimates of the adiabatic triplet energies are in excellent agreement with available experimental data.[12−16,30−35] The triplet energies of the [*p*,*p*]-POs are in the range of 2.75−2.85 eV when ZPVE corrections are taken into account (otherwise, they are ~0.1−0.15 eV higher). Interestingly, the triplet energies in the [*m*,*m*]-PO derivatives are consistently somewhat larger than in the corresponding *para* compounds (differences on the order of 0.1−0.2 eV), a feature which should be kept in mind in the design of new materials; this is consistent with the higher LUMO energies and ensuing larger HOMO−LUMO energy gaps calculated for the former. Importantly, while the introduction of the PO substituents results in a systematic reduction of the triplet energy by 0.1−0.3 eV, with respect to the core units alone, these energies are still ~0.2−0.5 eV larger than those of the blue phosphors discussed in this study.

Table 6. Adiabatic Triplet Transition Energies of the Phosphine Oxide and Phosphorescent Compounds[a]

X	ΔE_{trip}[b]	ΔE^0_{trip}[b]	Expt.	ref(s)
2H	2.99	2.86	3.01	30
CH_2	3.01	2.87	2.94	14
O	3.15	2.99	3.12	13
S	3.14	2.97	3.01	31
SO_2	2.85	2.72	2.78	32
NH	3.15	3.05	3.05	33
FPt1	2.69	2.57	2.63/2.68	34/35
FIrpic	2.67	2.56	2.65/2.66	4/35
		[*p*,*p*]-POs		
2H	2.86	2.75	2.72	12, 15
CH_2	2.88	2.76	2.72[c]	14, 15
O	2.99	2.85		
S	2.99	2.83		
SO_2	2.74	2.63		
NH	2.93	2.80		
		[*m*,*m*]-POs		
2H	2.96	2.83		
CH_2	2.99	2.85		
O	3.14	2.99	3.14	13, 16
S	3.11	2.95	3.07	16
SO_2	2.75	2.63	2.60[d]	
NH	3.16	2.97	2.97[e]	16

[a] All values are in eV. [b] ΔE_{trip} and ΔE^0_{trip} represent the adiabatic triplet transition energies without and with zero-point vibrational energy correction, respectively. [c] The experimental study was conducted on 2,7-bis(diphenylphosphine oxide)-9,9-dimethylfluorene. [d] Data taken from a yet-to-be-published work by P. A. Vecchi, L. S. Sapochak, and co-workers. [e] The compound studied experimentally was based on *N*-ethyl-carbazole.

To understand the nature of the triplet state in the PO derivatives better, in Figure 6, we compare the frontier molecular orbitals of the core units at the optimized geometries of the ground state and T_1 state. In the S_0-state, the biphenyl, dibenzofuran, dibenzothiophensulfone, and fluorene HOMOs have a nodal plane between the two phenylene rings, whereas, in carbazole and dibenzothiophene, HOMOs have nodes at the *para* carbons of each phenylene ring. At the T_1-state geometry, however, the HOMO consistently presents the same shape for all the core molecules due to the reordering of the HOMO and HOMO-1 levels in both carbazole and dibenzothiophene; this orbital reordering is also found for all their PO derivatives; the only exception is the [*p*,*p*]-carbazole PO derivative where the HOMO and HOMO-1 are mixed and transform into two new MOs (see Tables S3 and S4 in the Supporting Information).[36] On the other hand, the nature of LUMO remains the same when going from the S_0 state to T_1 state. In addition, the T_1 state of all the molecules studied in the present work including the [*p*,*p*]-carbazole PO compound, predominantly corresponds to a HOMO-to-LUMO transition (more than ca. 80%; see Table S5 in the Supporting Information). Therefore, as a result of the similar nature of the HOMO/LUMO wave functions at the T_1-state geometry, all the

---

(30) Wagner, P. J. *J. Am. Chem. Soc.* **1967**, *89*, 2820.
(31) Terada, T.; Koyanagi, M.; Kanda, Y. *Bull. Chem. Soc. Jpn.* **1980**, *53*, 352.
(32) Jenks, W. S.; Lee, W.; Shutters, D. *J. Phys. Chem.* **1994**, *98*, 2282.
(33) Bonesi, S. M.; Erra-Balsells, R. *J. Luminesc.* **2001**, *93*, 51.
(34) D'Andrade, B.; Forrest, S. R. *Chem. Phys.* **2003**, *286*, 321.
(35) American Dye Source, Inc., Quebec, Canada.

(36) We note that the structure with parallel P=O bonds, which is nearly as stable as the one with antiparallel P=O bonds (energy difference is ca. 46 meV), displays the same HOMO and HOMO-1 characteristics. Also, calculations with larger basis set (TZVP) of triple-ζ quality provide the same results.

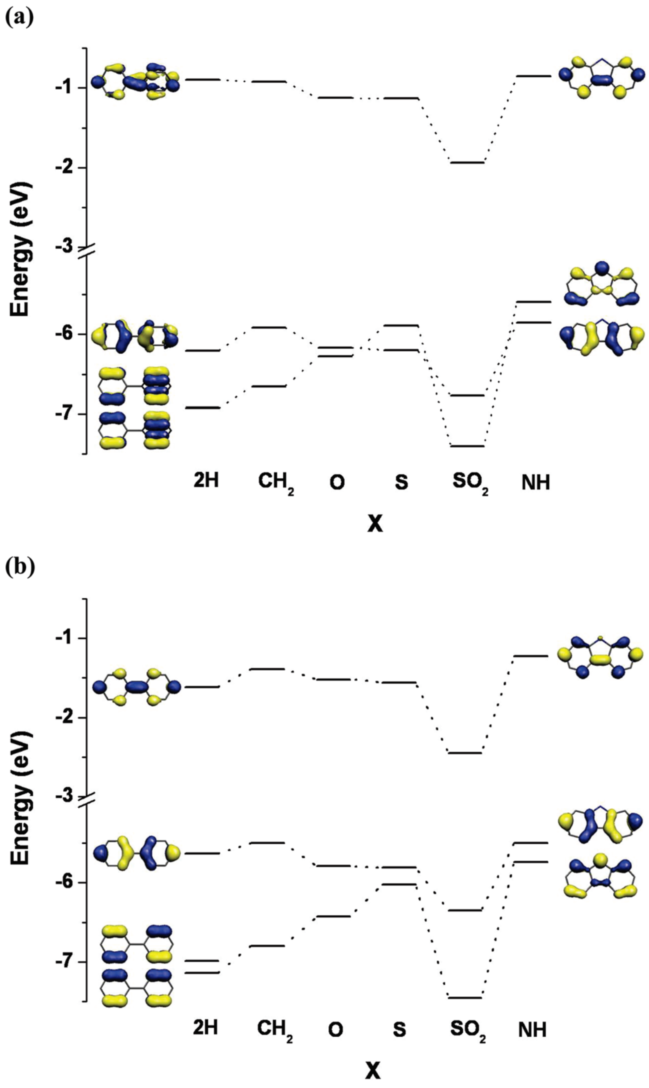

Figure 6. Comparison of the frontier molecular orbitals of the core molecules: (a) at the ground-state (S_0) geometry and (b) at the lowest triplet-state (T_1) geometry.

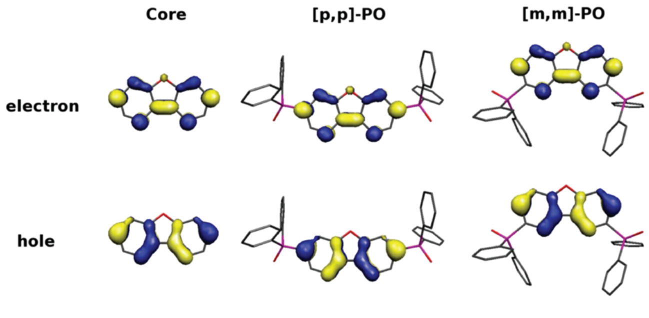

Figure 7. Natural transition orbitals (NTOs) for the lowest triplet transition of the dibenzofuran molecule and its bis(diphenylphosphine oxide) derivatives (the associated NTO eigenvalues are 0.9480, 0.9554, and 0.9431, for dibenzofuran and its *para* and *meta* PO derivatives, respectively).

molecules display T_1-states with almost-identical characteristics.

The natural transition orbitals (NTOs) associated with the T_1-state were also evaluated; as a typical example, those for dibenzofuran and its PO derivatives are displayed in Figure 7. The NTO analysis emphasizes that the PO derivatives exhibit T_1 transitions of exactly the same nature as their core units. This confirms that the phosphine oxide substitution does not alter the T_1-state characteristics of the core molecule; this is consistent with the negligible geometric deformations of the core unit in the T_1 state of the PO derivatives and the comparable triplet energies of the core molecules and their PO derivatives.

IV. Synopsis

We have investigated the relationship between the structure and the electronic/photophysical properties in a series of bis(diphenylphosphine oxides) that can be used as host materials in the emissive layers of blue PhOLEDs. The theoretical results confirm the picture drawn from experiment: the photophysical properties of the PO derivatives are similar to those of core molecules; the triplet energies are almost constant along the series; and the stabilization of both the HOMO and LUMO energies upon substitution is expected to lead to better hole-blocking properties and enhanced electron injection, respectively. The quality of the theoretical approach is verified by the excellent agreement found between the experimental UPS and IPES data and the simulated spectra.

In addition, the results of the calculations highlight the following features:

(i) In all the molecules considered in this study, the T_1-state presents the same character and corresponds to a LUMO−HOMO transition localized on the core moiety. At their optimized T_1-state geometries, the HOMOs and LUMOs of all the molecules present similar wave functions (with the exception of the [*p*,*p*]-carbazole PO derivative for which the HOMO and HOMO-1 levels are mixed). These findings are consistent with the observed similar triplet exciton energies, whatever the identity of the core molecule.

(ii) While the two patterns of PO substitutions (*para* vs *meta*) make little difference, in terms of modulation of the HOMO energies, they affect the LUMO energies much more markedly, because of the larger extent of (electron-withdrawing) mesomeric contributions in the *para* than *meta* compounds. This feature is also related to the slightly but consistently higher triplet energies calculated for the *meta* derivatives.

Thus, the results of our calculations underline that phosphine oxide derivatives provide a fertile ground for the design of appropriate host materials for PhOLEDs.

Acknowledgment. This work has been supported by Solvay and by the National Science Foundation (through the STC Program, under Award Number DMR-0120967). Work at Princeton was supported by the National Science Foundation (DMR-0705920) and the Princeton MRSEC of the NSF (DMR-0819860). Work at Pacific Northwest National Laboratory was supported by the Solid Sate Lighting Program of the U.S. Department of Energy (within the Building Technologies Program, Award No. M68004043) and managed by the National Energy Technology Laboratory. Pacific Northwest National Laboratory is operated by

Battelle Memorial Institute for the U.S. Department of Energy (under Contract No. DE-AC06-76RLO 1830).

Supporting Information Available: The Supporting Information includes the geometry parameters for dibenzofuran and its derivatives in the ground and lowest triplet excited (T_1) states; the HOMO and HOMO-1 wave functions of dibenzothiophene, carbazole, and their derivatives in the ground and T_1 states; the contributions of the HOMO-to-LUMO transitions to the lowest triplet states for the molecules investigated in this work. This information is available free of charge via the Internet at http://pubs.acs.org/.